

# We are IntechOpen, the world's leading publisher of Open Access books Built by scientists, for scientists

6,900

Open access books available

186,000

International authors and editors

200M

Downloads

Our authors are among the

154

Countries delivered to

TOP 1%

most cited scientists

12.2%

Contributors from top 500 universities



WEB OF SCIENCE™

Selection of our books indexed in the Book Citation Index  
in Web of Science™ Core Collection (BKCI)

Interested in publishing with us?  
Contact [book.department@intechopen.com](mailto:book.department@intechopen.com)

Numbers displayed above are based on latest data collected.  
For more information visit [www.intechopen.com](http://www.intechopen.com)



# Cell Growth Measurement

*Ning Xu, Xingrou Chen, Jingjing Rui, Yan Yu, Dongshi Gu,  
Jennifer Jin Ruan and Benfang Helen Ruan*

## Abstract

The cell is the basic structural and functional unit of all living organisms. As the smallest unit and building blocks of life, cells differ in size, shape, metabolism, reproduction, and growth requirements. Cells reproduce through cell division involving a four-phase (G1, S, G2, M) cell cycle, which is tightly regulated at multiple checkpoints. The resulting growth curve demonstrates that cell population increases in three sequential steps: incubation, exponential hyperplasia, and stagnation/death phases. Cell growth is subject to changes in disease state and/or environmental conditions. This chapter will focus on methods for cell growth measurement, which are grouped into five sections: cell cycle, apoptosis, growth curve, drug-induced proliferation (DIP), and continuous assays. Among the continuous assays, the EZMTT dye allows for long-term tracking of cell growth under various conditions and shows promise in precision medicine by early detection of drug resistance.

**Keywords:** cell cycle, apoptosis, growth curve, drug-induced proliferation, continuous assays, drug resistance

## 1. Introduction

The cell is the smallest unit of living organisms [1] and grows both in population and size. Cellular growth [2] is tightly regulated and usually shows three sequential steps, including incubation, exponential hyperplasia, and stagnation/death phases [3]. Unrestricted cell growth causes cancer, and drugs cure the disease by regulating the cell growth back to normal. Therefore, precise measurement of cell growth is very important in biomedicine, including cancer, aging, drug resistance, drug discovery, environment contamination, material biocompatibility [4, 5], fermentation, immunology, etc.

Cells grow by cell division which includes four major components: the G1, S, G2, and M phases in sequence [6], as shown in **Figure 1**. The signature of the G1 phase is the synthesis of enzymes that are required for DNA replication. During the S phase, DNA is replicated to produce two identical sets of chromosomes. The G2 phase is mainly involved in the production of microtubules that are required during the process of division, the mitotic phase. Increases in cell volume are observed during the interphase (G1, S, G2 phase). The M phase consists of prophase, metaphase, anaphase, and telophase in sequence, and the parent cell is divided into two daughter cells through nuclear division (karyokinesis), cytoplasmic division (cytokinesis), and formation of a new cell membrane [7].

Cell division is more complex in eukaryotes whose cell division involves either mitosis or a more complex process called meiosis. Mitosis and meiosis are two

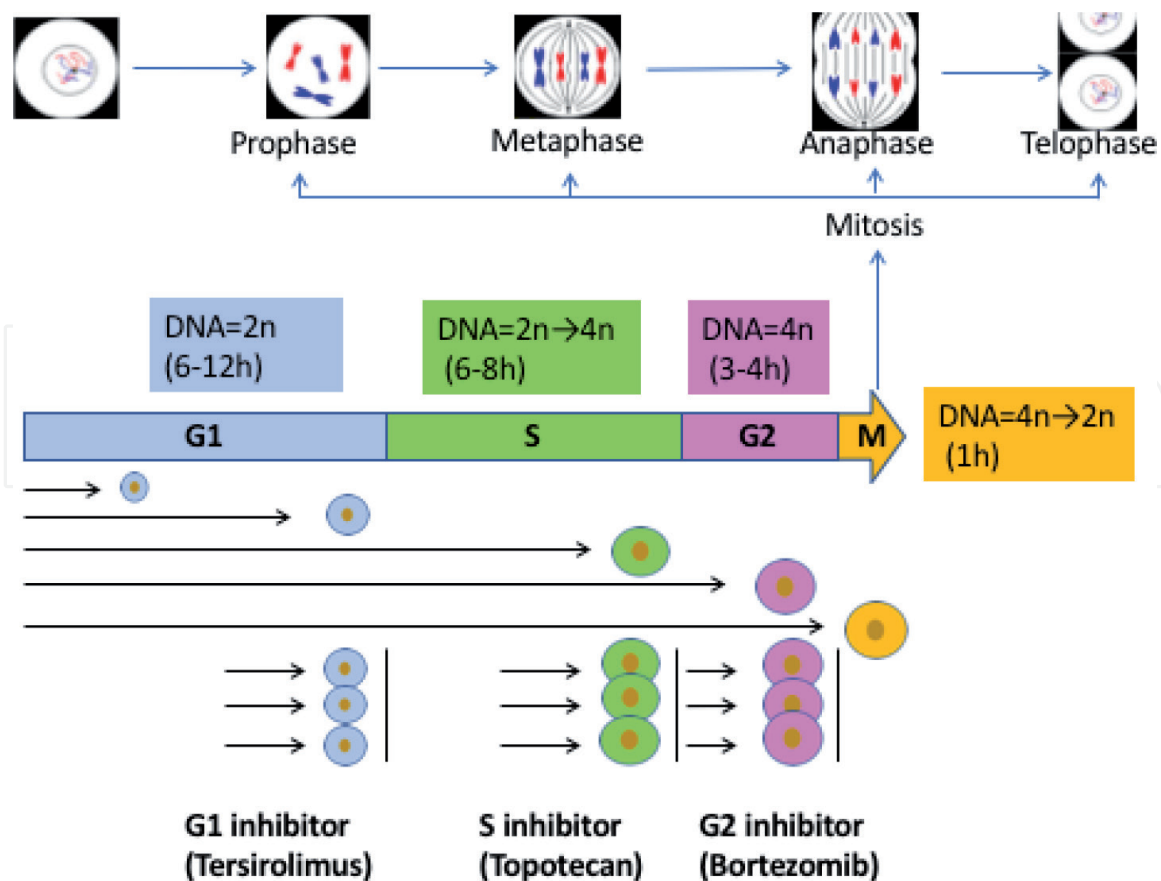


**Figure 1.**  
Cell cycle.

different “nuclear division” processes. Through binary fission, mitosis [8] produces two daughter cells with the same number of chromosomes as the parental cell. Meiosis, also called reductive division, is the division of a germ cell involving two fissions of the nucleus to form four gametes that have half the normal cellular amount of DNA. A male and a female gamete can then combine to produce a zygote, a cell which again has the normal number of chromosomes [9]. Therefore, the enlargement of cell volume and changes in DNA content are two parameters commonly used in cell cycle measurement.

The cell cycle is tightly regulated at multiple checkpoints [10]. Various growth conditions such as the temperature, nutrients, cell density, and drug treatment can block the cell cycle at various stages. Instead of unrestricted growth, the cell growth curve shows that the cell population increases through three phases: incubation period → exponential hyperplasia → stagnation period. During exponential growth, cells demonstrate great variation in required cell density and doubling times that are highly dependent on cell type and growth conditions.

Cell death occurs in each generation. Acute cellular injury causes traumatic cell death (necrosis) [11], whereas apoptosis is a highly regulated and programmed cell death that occurs each day in multicellular organisms. The average adult human loses between 50 and 70 billion cells each day due to apoptosis [12] which is critical, because uncontrolled cell proliferation is closely related to the occurrence of human diseases such as tumors. Commonly used analyses for apoptosis are morphological analysis, detection of apoptotic biomarkers, and flow cytometric analysis of cellular DNA content.

Inhibiting cancer cell or infectious microbial growth is the purpose of drug treatment. However, drug resistance is the notorious worldwide crisis that prolongs hospital stays and considerably increases mortality. Identification of specific genetic mutations has been the major effort in understanding drug resistance, but the

results have had little diagnostic value [13]. Recently, many research groups [14–17] demonstrated that drug resistance develops owing to a small population of cells resistant to the drug, and drug treatment results in the selection for the growth of the small drug-resistant cell population. Recognition of partial efficacy is, therefore, very important in early detection of drug resistance.

Traditionally, the dose–response curve is used to evaluate the potency of an inhibitor ( $IC_{50}$ ). Commonly used cell proliferation assays are metabolic activity-based methods such as the tetrazo-based cellular NAD(P)H detection system (MTT, CCK8, EZMTT) and the cellular ATP detection system (CellTiter-Glo Assay). Unfortunately, due to experimental error, the endpoint assays are not sensitive enough to detect the survival of a minor population of cells.

For precise measurement of drug efficacy, the drug-induced proliferation (DIP) rate has been proposed as a better parameter than the  $IC_{50}$  or MIC (80% inhibition) measurement [15]. However, the measurement of a precise DIP rate calls for continuous assays that can be used easily with various cell types.

Therefore, this chapter will mainly discuss the methods used for measuring cell cycle, apoptosis, growth curve, and drug-induced proliferation, continuous assays that can track the growth condition-induced cell proliferation, and its applications in early discovery of drug resistance.

## 2. Cell cycle

Each cell cycle involves the G1, S, G2, and M phases in sequence, and each phase is associated with its signature protein biomarkers, DNA content, and cell size, as shown in **Figure 1**. DNA ploidy and protein biomarker analyses are commonly used in cell cycle studies and have important applications in clinical cancer diagnosis, drug efficacy evaluation, prognosis prediction, cell dynamics, and apoptosis.

### 2.1 Parameters used for DNA content analysis

DNA ploidy, DNA index (DI), S phase fraction (SPF), and potential doubling time ( $T_{pot}$ ) are commonly used parameters for cell cycle analyses.

DNA ploidy refers to the number of chromosomes or the total DNA content in cells. DNA ploidy analysis in combination with clinical pathological diagnosis has a great value in early diagnosis and in prognosis prediction for malignant tumors, for both solid tumors and cancer cell extracts from body fluids, glandular secretions, and exfoliated tissue cells. Aneuploid tumors showed significantly higher recurrent rates than the diploid ones [18].

The DNA index (DI) refers to the ratio between the cells in G0/G1 peak of the tumor samples and that of the normal diploid samples. The calculation equation is  $DI$  (DNA index, number of judgment ploidy) = (average number of G0/G1 phase cell peaks in sample) / (average number of G0/G1 phase cell peaks in normal diploid cells). A DI of 1 means a normal diploid sample (generally the normal range is 0.9 to 1.1) [19].

The S phase fraction (SPF) shows the percentage of cells in S phase and indicates the proliferative activity of the cells. The calculation equation is  $SPF$  (S phase fraction %) =  $S$  cells / ( $G0/G1 + S + G2M$ ) cells  $\times 100\%$ . Another cell proliferation parameter is proliferation index (PI), and the calculation equation is  $PI$  (proliferation index %) = ( $S + G2M$ ) cells / ( $G0/G1 + S + G2M$ ) cells  $\times 100\%$ .

The potential doubling time ( $T_{pot}$ ) refers to the time required to double the cell number, which occurs during exponential growth.

## 2.2 DNA content analysis

DNA content can be analyzed after fluorescent staining or labeled nucleic acid incorporation as shown in **Table 1**.

As shown in **Figure 2**, DAPI and Hoechst dyes penetrate the membrane and are commonly used to label live cells, whereas propidium iodide (PI), propidium monoazide (PMA), and ethidium bromide monoazide (EMA) only label dead cells. Newly synthesized DNA in active proliferating cells can be labeled by the radiolabeled  $^3\text{H-TdR}$ ,  $^{125}\text{IUdR}$  [24], or the fluorescent-labeled BrdU and EDU [25].

Flow cytometry measurement (FCM) is a sensitive method to measure cell size and fluorescent labeling. Double staining both cellular DNA and protein biomarker allows identification of cells in G1 peaks, G2+ M peaks, and S platforms, as well as the subdiploid peaks (apoptotic peaks) before the G1 peak. These methods in combination with other biomarkers show the distribution of cells in each phase of the cell cycle and can be used to investigate cell dynamics [26].

## 2.3 Protein biomarkers

Proteins that are found in proliferating cells, but not in nonproliferating cells can be used as biomarkers for cell cycle measurement. Ki-67 protein (also known as MKI67) is present during all active phases of the cell cycle (G1, S, G2, and mitosis) but is absent in resting (quiescent) cells (G0) [27]. During interphase, the Ki-67 protein is exclusively located in the cell nucleus, whereas in mitosis most of the protein is relocated to the surface of the chromosomes. During cell progression through S phase of the cell cycle, the Ki-67 protein markedly increases [28]. As shown in **Figure 1**, the fluorescent-labeled monoclonal Ki-67 antibody has been used for cell cycle measurement and cancer diagnosis. Other commonly used cell proliferation biomarkers include proliferating cell nuclear antigen PCNA [29], topoisomerase IIB [30], and phosphorylated histone H3 [31].

DNA stain	Principle	Membrane permeability	Function
4',6-diamidino-2-phenylindole (DAPI)	Binds to DNA A-T rich region [20]	Yes	Live cell
Hoechst dye	Binds to DNA A-T rich region [21]	Yes	Live cell
Propidium Iodide (PI)	Label dead cells [22]	No	Dead cell
Propylene glycol monomethyl ether acetate (PGMEA)	In combination with dsDNA to form a stable and strong covalent nitrogen-carbon bond [23]	No	Dead cell
Ethidium bromide monoazide (EMA)	Covalent cross-linking with genomic DNA [23]	No	Dead cell
$^3\text{H-TdR}$ incorporation	$^3\text{H-TdR}$ incorporates in DNA synthesis	Yes	Live cell
$^{125}\text{IUdR}$ incorporation	$^{125}\text{IUdR}$ incorporates in DNA synthesis	Yes	Live cell
BrdU incorporation	BrdU participates in DNA synthesis in cell proliferation	Yes	Live cell
EDU incorporation	EDU participates in DNA synthesis in cell proliferation	Yes	Live cell

**Table 1.**  
*Comparison of methods for DNA labeling.*

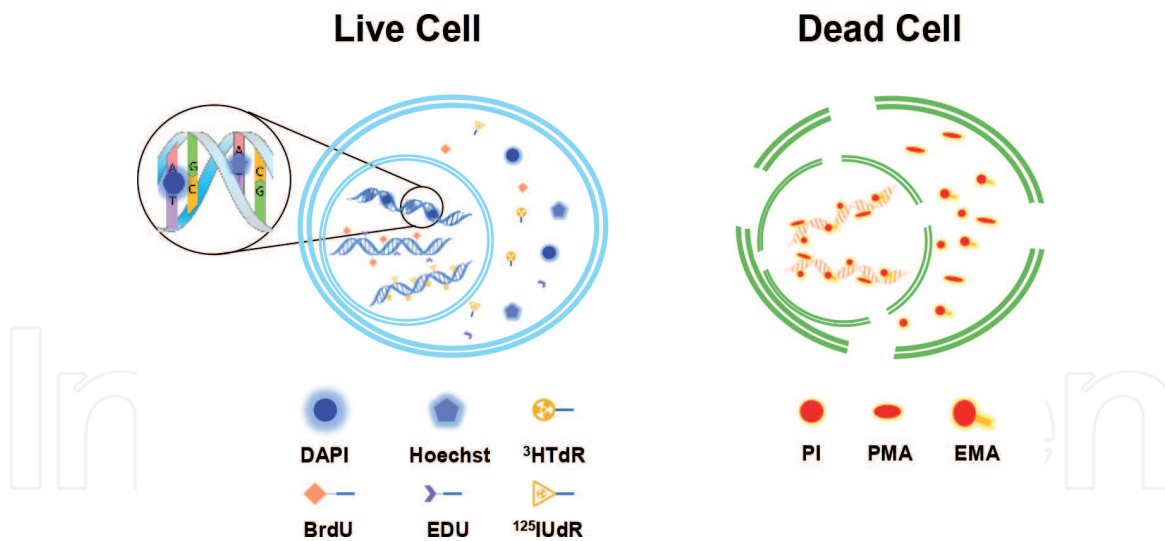


**Figure 2.**  
*Methods for DNA analysis in both live and dead cells.*

### 3. Apoptosis

Apoptosis is a programmed cell death, and the process involves a series of morphological changes such as blebbing, cell shrinkage, nuclear fragmentation, chromatin condensation, as well as biochemical changes such as chromosomal DNA fragmentation, global mRNA decay [32], and appearance of protein biomarkers in protein degradation pathways.

Commonly used analyses include transmission electron microscopy for morphological analysis, biochemical assays for detection of apoptotic biomarkers, and flow cytometry analysis of cellular DNA content (**Figure 3**).

#### 3.1 Transmission electron microscopic analysis

Tissue or cells can be directly stained using dyes such as hematoxylin, methyl green pyronine, and acridine orange for microscopic analysis. Under the transmission electron microscope [33], apoptotic cells show reduced size and more concentrated cytoplasm. In the nucleus of pro-apoptosis phase, the chromatin is highly coiled, and many vacuole structures called cavitation appear; in the phase IIa nucleus, the chromatin is highly coagulated and marginalized; in the end, the nucleus is cleaved into fragments and produces apoptotic bodies. Fluorescence microscopy and confocal laser scanning microscopy [34] can also be used to observe the progress of apoptosis, based on morphological changes of nuclear chromatin DNA-specific dyes such as Hoechst dye series and DAPI.

#### 3.2 TUNEL method

The TUNEL assay [35] distinguishes between normal and apoptotic cells based on the amount of FITC-dUTP incorporation into the broken DNA ends in the intact single apoptotic nuclei or apoptotic bodies, whereas the normal or growing cells have almost no DNA breaks and will not be stained. This method accurately reflects the most typical biochemical and morphological features of apoptosis and can be used with paraffin-embedded tissue sections, frozen tissue sections, cultured cells, and tissue-separated cells. The method is simple, easy, and sensitive in detecting a very small amount of apoptotic cells.

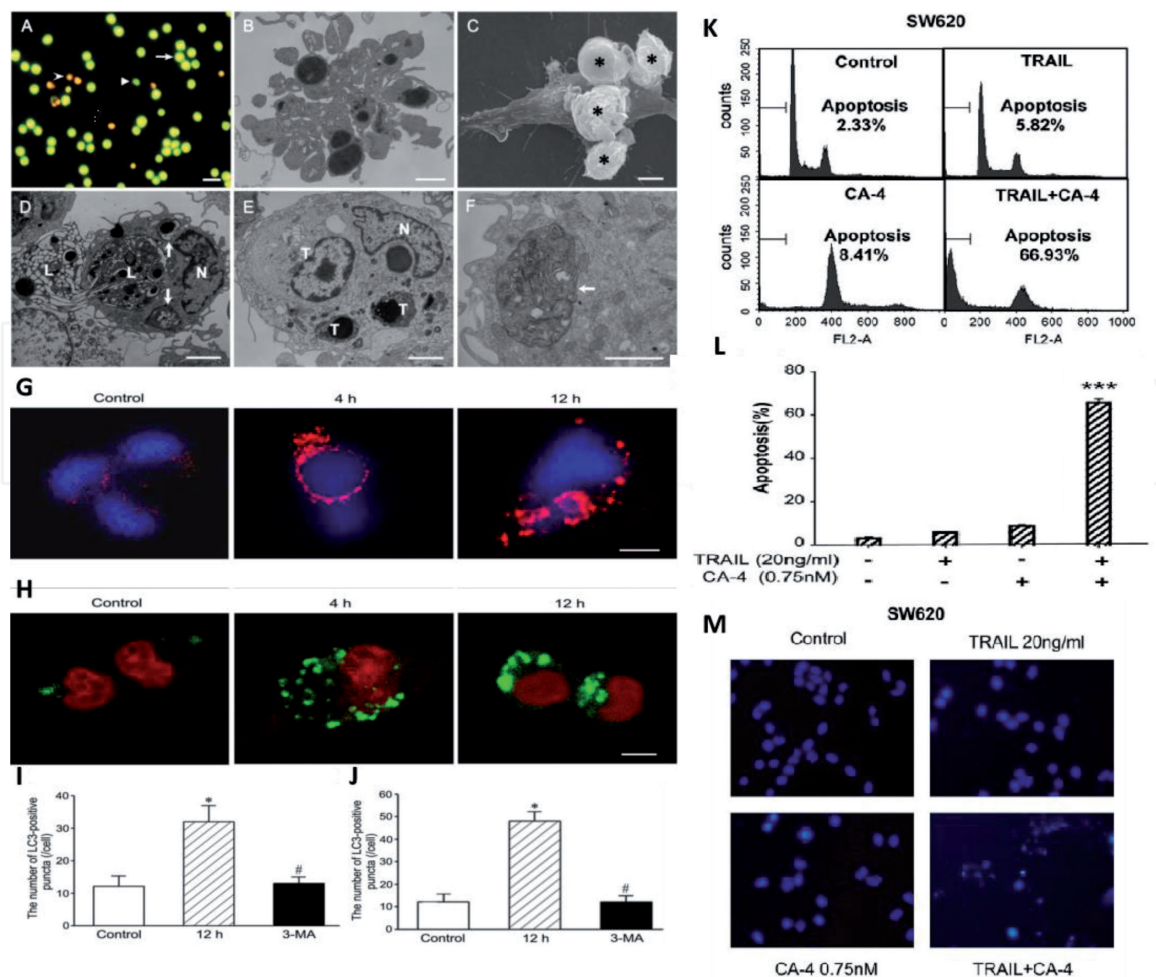


**Figure 3.**

*Methods in measuring apoptosis: (A) lymphocytes stained with EB/AO solution. Triangle, arrow, and arrowhead show viable, early apoptotic and late apoptotic cells, respectively. (B) Transmission electron image of a broken apoptotic lymphocyte. The cell breaks up into apoptotic bodies containing organelles or the condensed nuclear fragments. (C) Scanning electron image of a macrophage phagocytosing the apoptotic lymphocytes (asterisks). (D) A macrophage engulfing an apoptotic lymphocyte L, containing the condensed nuclear fragments. Arrows show phagosomes containing the apoptotic bodies of lymphocytes. (E, F) A macrophage phagocytosing apoptotic cells. (G–J) LC3 fluorescent stain in macrophages phagocytosing the apoptotic lymphocytes. The nuclei were stained with DAPI (G) or PI (H). (K and L) PI staining was used to evaluate the apoptosis.*

The limitations of the TUNEL method are as follows. Firstly, it labels apoptotic cells only in the middle and late stages. Secondly, necrotic cells also contain DNA breaks and are labeled by dUTP, so the assay is not specific enough to distinguish between apoptotic and necrotic cells. Thirdly, cells need to be fixed during the labeling process, which may lead to excessive cell debris or loss of DNA fragments. Lastly, subjective factors are involved when counting the number of the apoptotic cells.

In addition, agarose gel electrophoresis can be used to detect the apoptotic DNA fragmentation into an integer multiple of 180–200 bp [36]. ELISA can be performed using anti-DNA and anti-histone monoclonal antibody to detect nucleosome fragments [37]. Mitochondrial membrane potential measurement can distinguish early apoptosis [38] and provides a nice complement to the TUNNEL method.

### 3.3 Fluorescent staining for flow cytometry analysis

Application of annexin V is a widely used method for detecting apoptosis [39]. Annexin V is a  $\text{Ca}^{2+}$ -dependent phospholipid binding protein with a molecular weight of 35–36KD, which can bind with phosphatidylserine with high

affinity. Annexin V can be labeled with fluorescein isothiocyanate (FITC, PE) or biotin and used as a fluorescent probe to detect apoptosis by flow cytometry or fluorescence microscopy.

PI dye does not pass through the intact cell membrane, but in the middle and late stages of apoptosis, PI can pass through the cell membrane to bind to the DNA and redden the nucleus [40, 41]. PI staining of the apoptotic cells shows a subdiploid peak (Ap peak) that appears before the G1 peak. The number of apoptotic cells can be detected based on the level of the Ap peak. Therefore, combining results from both annexin V staining and PI staining, cells in the early and late stage of apoptosis and necrosis can be distinguished.

However, the limitation of both staining methods is the poor sensitivity. It is difficult to detect DNA fragments in early apoptotic cells and easy to miss the detection of apoptotic cells in S phase or G2/M phase. Meanwhile, the PI method is partially necrotic, and the cellular debris could cause false detection.

Additional methods are detecting the release cytochrome C from mitochondria into cytoplasm during apoptosis [42], as well as activation of signaling pathways involving caspase 3, caspase 9, Apaf-1, PARP, Bcl2, Akt, TFAR19, etc., to differentiate the exogenous or endogenous cause of cell apoptosis [43].

### 3.4 Double or multiple staining

To distinguish the apoptotic cells, necrotic cells, and living cells, researchers perform flow cytometric analysis after double staining with annexin V and PI. Annexin V-FITC has poor membrane permeability and can specifically bind phosphatidylserine; for live cells, no phosphatidylserine can be detected by annexin V, but during apoptosis, phosphatidylserine is valgus outward to the outer side of the cell membrane for easy detection. The fluorescent dye PI binds to chromatin but does not enter the cytoplasm of live cells. However, PI can enter the apoptotic cells and necrotic cells and effectively stain the concentrated chromatin in apoptotic cells. In addition, for low PI-stained cells, H0342 dye can be used for detection of apoptotic cells with concentrated chromatin. H0342 stain enters cells with intact membranes and stains apoptotic cells more strongly than normal cells. When used in combination with forward scatter (FSC) and side scatter (SSC), H0342 staining can distinguish apoptosis from living cells [44].

Taken together, the FCM method requires less sample, provides high sensitivity, and simultaneously analyzes apoptotic cells and normal cells. Morphological observation can be carried out using an optical microscope, and electron microscopy is an authoritative method, which is commonly used before serious quantitative analysis. Agarose gel electrophoresis can also be used as a qualitative analysis, but the results need further confirmation by TUNNEL technology or annexin-V/PI dual-label method.

## 4. Cell proliferation

Cell growth (proliferation) can be evaluated by the time-dependent changes of the total number of proliferating cells, as well as the ratio of cells among individual phases of the cell cycle. The cell growth curve was plotted to show the time-dependent increase in cell numbers. Depending on the cell type and growth condition, the required cell density to enter the exponential phase and the rate of cell growth measured by the doubling time ( $T_{pot}$ ) could be very different. For example, most microbials (e.g., *E. coli*) enter the exponential growth phase with low cell numbers and show fast growth rate with a doubling time less than an hour [45],

whereas *M. tuberculosis* and mammalian cells have longer doubling time of several hours or a day. The growth and reproduction of cells can be further altered by changes in temperature, nutrition, viral infection, and/or the presence or absence of inhibitors [46]. Therefore, the growth curve is important in guiding clinical drug usage, investigating gene functions, and understanding drug mechanism of action. Various methods have been developed to measure the absolute number of cells or the changes in cell number, as shown in **Figure 4**.

#### 4.1 Manual cell counting

Traditionally, cell numbers are counted by taking an aliquot of a homogenous cell suspension and plating on a hemocytometer to count the numbers under a light microscope. The obtained cell number in a certain volume of the suspension is then converted into the cell concentration (cells per ml) in the stock solution. Bacteria are counted by a Petroff-Hausser bacterial counter, a Hawksley counter, and/or the plate colony formation method. The plate colony counting method often gives a lower cell number than the actual value, because it is often difficult to disperse bacteria into a single cell and to make sure that a single colony is not derived from several bacteria.

#### 4.2 Automated mechanical counting

The most commonly used automatic cell counting methods are direct electrical impedance, flow cytometry, computer-aided image analysis, and serological counting. Through changes in electrical properties, the direct electrical impedance method quantifies the number and the volume of cells in the blood. Using a photomultiplier to filter and detect the signal, flow cytometry records both the density and height of fluorescent pulses and then converts them to the number of bacteria; the method is fast and sensitive and can simultaneously analyze the cell morphology and protein biomarkers. Computer-aided image analysis [47] and serology [48] counting methods analyze the image or 2D picture to obtain accurate quantification and morphological structure. So far, both methods have been used successfully in biology, materials science, mineralogy, and neurological science.

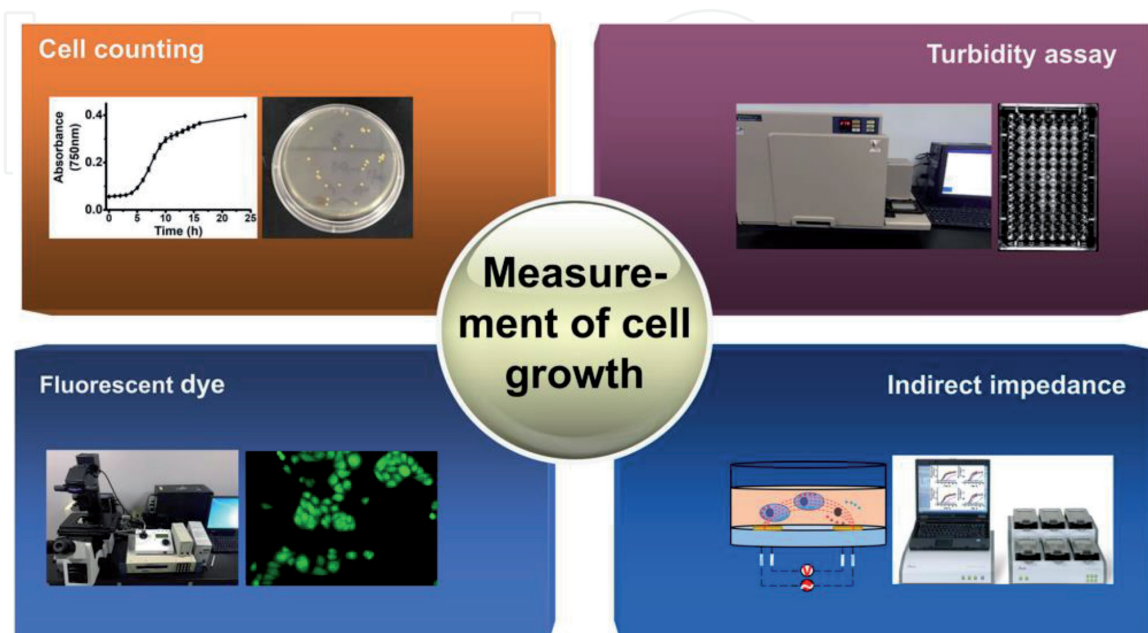


**Figure 4.**  
The main methods for cell growth measurement.

### 4.3 Indirect cell counting methods

#### 4.3.1 Turbidity assay by spectrophotometry

Turbidity can be observed when the cell density reaches certain level; within a certain range, the number of cells is proportional to the turbidity of the bacterial culture. The cell turbidity is measured by a spectrophotometer or a colorimeter, and a standard curve is generated by plotting the absorbance at OD600nm and the actual cell numbers in the sample. Photoelectric turbidimetric counting is a simple, rapid, and continuous measurement suitable for high-throughput screening. However, its optical density is less sensitive, cannot differentiate between dead or live bacteria, and is greatly affected by cell size, morphology, and the color of the culture solution [49].

#### 4.3.2 BACTEC MGIT method

BACTEC MGIT [50, 51] measures microbial growth by oxygen depletion which requires anaerobic conditions, so the bacteria must be grown in a sealed tube or compartment. This method has been widely applied in medical diagnosis but is not suitable for high-throughput plate-based AST assays.

#### 4.3.3 Fluorescent dye method

Live or dead cells that cannot be differentiated by the light microscope can be counted after fluorescent labeling. **Table 2** showed the commonly used dyes that

Fluorescent dye	Stain subject	Membrane permeability	Excitation/ emission wavelength	Function	Detection
SYTO nucleic acid stains	Nucleic acid [52]	Yes	420~657/441~678	Live or dead cell	Fungus, bacteria
SYTOX green nucleic acid stain	Nucleic acid [53]	No	~504/~523	Dead cell	Fungus, bacteria
Propidium iodide (PI)	Nucleic acid [54]	No	~530/~635	Dead cell	Fungus, bacteria, mammals
Sulforhodamine B (SRB)	Protein [55]	Yes	~565/~586	Live cell	Mammals
PHK26, 67	Membrane [56]	Yes	~551/~567, ~496/~520	Live cell	Mammals
DiO	Membrane [57]	Yes	482~487/ 501~504	Dead cell	Mammals
DiD	Membrane [58]	Yes	~646/~665	Dead cell	Mammals
Calcofluor white M2R	Cytoderm [59]	Yes	385~405/ 437~445	Live cell	Fungus
DiBAC4(3)	Membrane [60]	Yes	506/ 526	Dead cell	Fungus, bacteria, mammals

**Table 2.**  
 Summary of fluorescent dye.

label the cellular components such as nucleic acid, cytoplasm, cell membrane, redox environment, and lipase. For example, SYTO series nucleic acid fluorescent dyes, etc. stain the DNA or RNA of the live or dead cells; PI nor SYTOX Green nucleic acid dyes cannot transfer into the live cells and stain the DNA of the damaged cell membranes. Both types of dyes can be used in combination to measure the ratio of live and dead cells. After labeling, the cells can be detected by a fluorescence microscopy or by a flow cytometry. The combination of fluorescent dyes and advanced instruments makes it possible to realize the “visualization” and investigate the mechanisms of action under the physiological and pathological conditions and to explain the significance of life effects, which is of great significance in the field of disease diagnosis and drug screening.

## 5. Drug-induced proliferation assays

A drug is a substance that induces functional changes in an organism through chemical or physical actions, regardless of whether the resulting effect is beneficial or detrimental to the health of the receiving organism. Therefore, assays are critical in revealing interactions between the drug and the organism. In particular, the cell proliferation assays provide valuable information for exploring the pathogenesis of the disease, diagnosing the disease, and treating the disease.

Traditionally, a dose–response curve is used to evaluate the potency of an inhibitor ( $IC_{50}$ ). The commonly used cell proliferation assays are either metabolic activity-based methods such as the tetrazo-based cellular NAD(P)H detection system (MTT, CCK8 method) or the cellular ATP detection system (CellTiter-Glo Assay). According to the mechanism of metabolic activity detection, these endpoint colorimetric and fluorescence methods can be divided into five categories (**Table 3**): the reducing environment of live cells, ATP of live cells, detecting products released by dead cells, esterase, and detecting mitochondrial metabolism of live cells.

### 5.1 Reducing environment of live cells

Resazurin and its derivative C12-resazurin are not fluorescent, but their reduced forms are fluorescent. Dehydrogenase reduces the non-fluorescent blue resazurin into a strongly fluorescent pink resorufin [61] in enzyme- or cell-based assays. Since the dehydrogenase level is high in active cells and very low in damaged or inactive cells, the resazurin assay shows a strong signal in metabolically active cells. Interestingly, even though resazurin can be reduced by mitochondrial enzymes, no evidence of resazurin reduction was found in mitochondria as shown by confocal microscopy analysis [62].

Resazurin is water-soluble and stable in culture medium. Single reagent addition allowed for simple assays of cell viability which is especially suitable for automated manipulation and high-throughput analysis [63]. However, the fluorescence is bleached by light, so it is not suitable to track the cell growth.

### 5.2 ATP production in live cells

Adenosine triphosphate (ATP) is an indicator of active live cells, and its cellular level directly reflects the number and state of cells. The CellTiter-Glo method is a luminescence-based endpoint assay, commonly used for ATP measurement after cell lysis. The assay is based on ATP consumption by luciferase to produce light (maximum emission wavelength ~560 nm at pH 7.8) [64]. Due to the absence of interference of endogenous luciferase in mammalian cells, a stable glow-type signal

Classification	Method	Description	Cell viability	Application
Reducing environment of live cells	Resazurin	Reduced by cytosolic dehydrogenase in metabolically active cells to produce pink strong fluorescent resorufin	Live cells	Growth
ATP production in live cells	CellTiter-Glo	Luciferase consumes ATP to produce light	Lysed cells	Growth
Esterase of live cells	FDA;calcein-AM	Cleaved by esterase in living cells to produce a fluorescent substance retained in the cell	Live cells	Division
Released products of dead cells	LDH release	LDH released by damaged or dead cells reduces the tetrazolium salts to colored formazan	Dead cells	Death
	<sup>51</sup> Cr release	<sup>51</sup> Cr released by damaged or dead cells can be measured by a radioactivity assay	Dead cells	Death
Mitochondrial dehydrogenase of live cells	Tetrazolium	Reduced by mitochondrial dehydrogenase to produce colored formazan products	Live cells	Growth

**Table 3.**  
 Comparison of commonly used methods for drug-induced proliferation assays.

generated using luciferase can be detected as little as 0.1 picomoles ATP by luminometers, showing high sensitivity, although the signal decreases after 10–30 min.

The luciferin-luciferase bioluminescence assay has been used to detect small amount of bacterial contamination in samples such as blood, milk, urine, soil, and sludge [65]. In addition, the assay can evaluate antibiotic effects, determine cell proliferation and cytotoxicity in both bacterial and mammalian cells [64], and distinguish the cytostatic and killing potential of anticancer drugs for malignant cell growth. Furthermore, it has been used for bioactive factor activity assays, large-scale antitumor drug screening, cytotoxicity assays, and tumor radiosensitivity assays.

### 5.3 Lactonase in living cells

Lactonase is a non-specific esterase and cleaves a non-fluorescent molecular probe to produce a fluorescent substance. Lactonase activity is high in live cells but low in dead cells, so the fluorescence is seen and retained in live cells. In addition, the fluorescence can be evenly distributed to the two daughter cells after cell division, although each successive passage decreased the fluorescence intensity in cells by 50% as analyzed by flow cytometry [66].

The most commonly used fluorescent probes are fluorescein diacetate (FDA) and its derivative succinimidyl ester of carboxyfluorescein diacetate, commonly known as CFSE-SE [67]. CFDA-SE was initially used for lymphocyte proliferation testing in 1994 and then applied to detect monocytes, fibroblasts, etc. The CFDA-SE method determines the cycle number of cell divisions based on fluorescence intensity. Also, it can be used to trace in vivo studies [68, 69].

In addition, calcein-AM, (3',6'-Di(O-acetyl)-4',5'-bis[N,N-bis(carboxymethyl)aminomethyl] fluorescein tetraacetoxymethyl ester), also known as calcein acetyl

ester, is a fat-soluble substance and membrane-permeable fluorescein dye [70]. It is non-fluorescent and freely enters the cytoplasm and organelles such as the mitochondrial matrix. Upon entry, calcein-AM can be hydrolyzed by intracellular esterase to produce water-soluble calcein (calcium chlorophyll), which remains in the cytosol and mitochondrial matrix and produces strong green fluorescence under 494 nm excitation light.

#### 5.4 Released products from dead cells

The radioisotope chromium ( $^{51}\text{Cr}$ ) release method was initially developed to detect dead cells and has now gradually been replaced by the LDH release method. Due to increased membrane permeability, the damaged or dying cells release the cytosolic LDH in cell culture medium [71], so the LDH activity is proportional to the number of dead cells. The LDH release assay has been used to measure the activity of cytotoxic lymphocyte (CTL) and natural killer (NK) cells, as well as the cytotoxicity caused by drugs, chemicals, or radiation.

#### 5.5 NADH and NADPH production of live cell

NADH and NADPH are important biological cofactors for enzymes that are fundamental for various biological processes, such as energy metabolism, mitochondrial function, oxidative stress, immunological functions, and cell death [72]. Antioxidant drugs that could change cellular NAD(P)H concentrations have been effective in diseases such as aging, inflammation, neural degeneration, and cancer [73, 74]. Many tetrazolium compounds can be reduced by NADH and NADPH to produce colored formazin and have been developed commercially for cell vitality assay, as shown in **Table 4** [75].

Triphenyl tetrazolium chloride (TTC) is a lipophilic and light-sensitive compound, and the TTC assay was developed back in 1894 for seed viability tests and is currently a traditional method for brain live-dead neuron evaluation after ischemic stroke [76]. MTT is the most commonly used reagent for cell proliferation or cell toxicity assays, but its formazan is water-insoluble and requires an additional DMSO solubilization step for its quantification at 540 nm [77]. WST-8 is a water-soluble tetrazolium salt, and its brown-colored formazan can be measured directly by UV absorbance at 450 nm. Because of its simple protocol, the WST-8 (CCK-8) assay has become a popular cell vitality method [78–80]. However, WST-8 is not very stable especially under the reduced condition, so EZMTT was developed for drug-induced proliferation assay [81]. EZMTT is another water-soluble tetrazolium salt which is

Tetrazolium	Structural formula	Solubility (tetrazolium/formazin)	Color (tetrazolium/formazin)	Cytotoxicity	Reagent stability
MTT	a	Soluble/insoluble	Yellow/purple	**	**
XTT	e	Soluble/soluble	Yellow/orange	****	****
MTS	i	Soluble/soluble	Yellow/purple	**	****
WST-1	l	Soluble/soluble	Yellow/orange	*	****
CCK-8/WST-8	t	Soluble/soluble	Yellow /orange OD 450 nm	*	***
EZMTT	o	Soluble/soluble	Yellow/orange OD 450 nm	Essentially nontoxic	**

\*less \*\*\*\* the most

**Table 4.** Comparison of MTT, XTT, MTS, WST-1, CCK-8, and EZMTT.

less toxic than also, EZMTT reagent showed excellent stability and signal of background ratio. Effort has been made to develop the EZMTT to greatly enhance the sensitivity and precision of the drug-induced proliferation assay.

In summary, these cell metabolism-based assays are commonly used as endpoint assays for  $IC_{50}$  measurement to rank the potency of a drug. However, the world crisis in drug resistance in infectious disease and cancer called for a deeper look at the drug-induced proliferation assays. Since drug resistance develops owing to a small fraction of the cell population that is resistant to the drug, a sensitive method for detecting partial drug resistance is very important in preventing the occurrence of drug resistance. Another approach is to measure not only the drug potency by  $IC_{50}$  values but also the drug efficacy by the drug-induced proliferation rate (DIP) [15]. However, to minimize the experimental error in detecting minor growth, precise DIP rate measurement in HTS mode requires the availability of a continuous assay that can track the cell proliferation from the same samples.

## **6. Continuous assay**

Continuously tracking the cell growth is important for accurate assessment of drug effects and/or growth condition changes. Even though various endpoint assays [75, 82, 83] can be terminated at various time point to obtain the time-dependent cell proliferation curve, the procedures are labor-intensive and have high experimental error. Therefore, a nondestructive continuous assay is highly desirable and critical for the precise evaluation of drug potency and efficacy. Besides the traditional turbidimetric assay by spectrophotometry that has been used for years in microbial assays, four new technologies have been developed that can be used for continuous assays.

### **6.1 High-content analysis**

High-content analysis is a cell imaging and analysis system which includes automatic high-speed microscopic imaging, fully automatic image analysis, and data management. Through snapshot cellular microscopic imaging of a 96-well plate followed by synchronous analysis, the high-content analysis, such as the CloneSelect™ imaging system, accurately measures the cell number without any cell damage. Compared with the MTT method, the experimental deviation of dose pharmacodynamic curve obtained by CloneSelect™ imaging system is smaller and more reproducible. Therefore, high-content analysis has become a reliable choice for big pharmaceutical companies to evaluate drug antiproliferation effects in high-throughput screening, although mostly for attached mammalian cells.

### **6.2 Electrical impedance technology**

Electrical impedance technology-based real-time cellular analysis (RTCA) [84–86] and Epic BenchTop optical biosensors methods [87, 88] have been used in measuring bacterial growth. However, the methods require cells to be cultured on the working electrode or a sensor array of complex structures. The methods [89] cannot detect changes in the cells themselves, so the cell damage caused by drugs and the understanding of the mechanism of drug action are difficult to assess accurately; this inevitably brings detection error and interference. In addition, the requirement of complex laboratory infrastructure further limits their utility.

### 6.3 Raman spectroscopy analysis

Raman spectroscopy provides a spectroscopic fingerprint of a substance. Based on the difference in monochromatic light with vibrational modes, Raman spectroscopy can be used for qualitative and quantitative measures of the changes in biochemical composition. For example, Raman spectroscopy was used as a noninvasive method to distinguish cells at different stages in the cell cycle [90]; to identify living cells from dead cells [91–95]; to image cellular organelles [96]; to track drug distribution [97] and metabolism [91]; to monitor cell apoptosis [94], death, and cytotoxicity [92, 95]; and to study cell responses to external stimuli [97–101]. However, the analysis of Raman results requires expertise in identifying the spectroscopic fingerprint of a substance.

### 6.4 EZMTT dye-based cell proliferation analysis

The EZMTT dye [81] was initially designed to overcome the stability issue of WST-8 (CCK-8) reagent which can cause false positives in the presence of antioxidants such as BME (**Figure 5A**) or EGCG. Later, the EZMTT dye was found to be essentially nontoxic and stable in various media [102]. After a single dye addition (**Figure 5B**), the EZMTT method showed linear dose–response to cell numbers and higher signal to background ratio than other relevant methods (**Figure 5C**). The  $IC_{50}$  values measured by the EZMTT method are precise and essentially the same as the other methods (**Figure 5D**). Interestingly, when both EZMTT and WST-8 (CCK-8) methods were applied to track the growth of

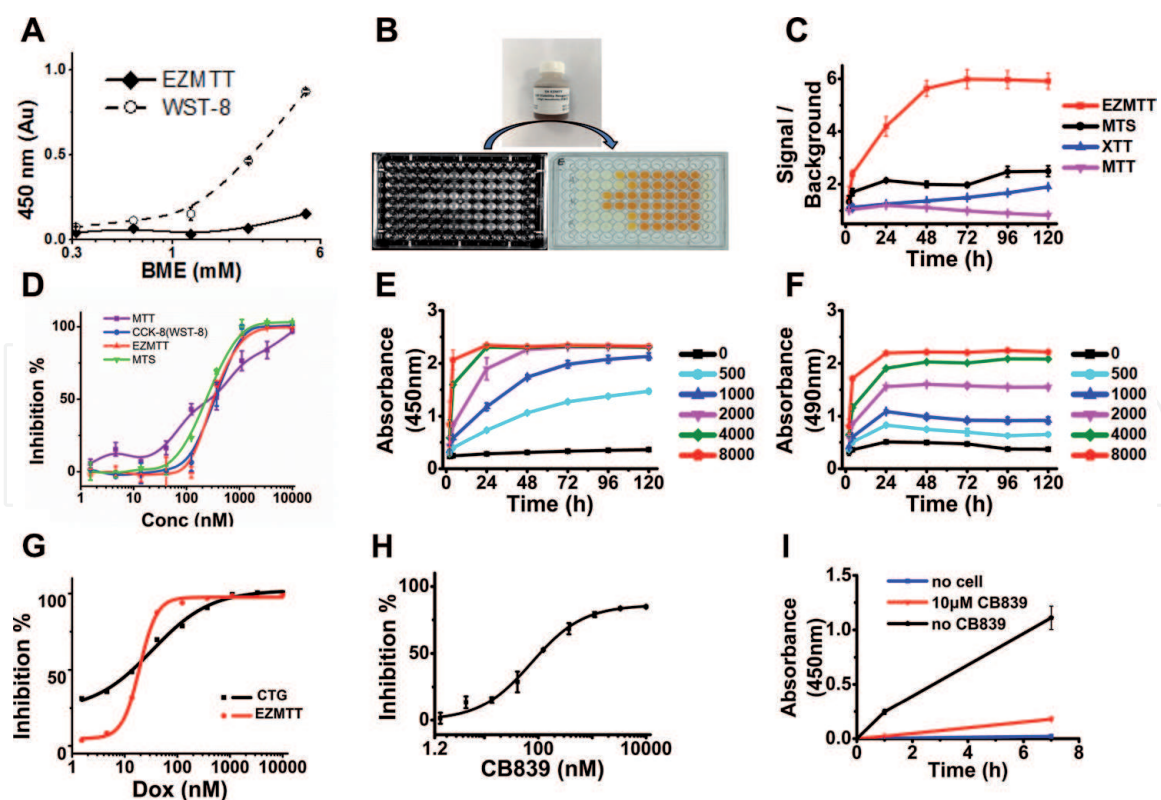


**Figure 5.**

*EZMTT assays: (A) EZMTT dye is stable in the presence of up to 6 mM BME. (B) One step addition of the EZMTT dye allows sensitive measurement of cell growth. (C) Comparison of the signal to background ratio of various tetrazo-based assay (MTS, MTT, CCK-8, EZMTT) in the presence of the same amount of A549 cancer cells. (D) Essentially the same  $IC_{50}$  values were obtained from the MTS, MTT, CCK-8, or EZMTT-based assays. (E) Cell growth followed by the EZMTT method. (F) Cell growth followed by the WST-8 method. (G) For a good inhibitor, essentially the same  $IC_{50}$  values were obtained from the CTG or EZMTT-based assays. (H) CB839 could only achieve up to 80% inhibition; (I) the DIP rate of CB839.*

A549 lung cancer cells, WST-8 (CCK-8)-treated cells stopped growth in 1 day, whereas the EZMTT-treated cells could grow till saturation (**Figure 5E and F**) and allowed easy determination of the cell density and the doubling time in the exponential phase.

In addition, when the EZMTT method was used to track the drug-induced proliferation (DIP) rate changes, the EZMTT method demonstrated high sensitivity and reliability in detecting drug resistance. **Figure 5H and I** compares the dose–response curve obtained by the CellTiter-Glo (CTG) method and the EZMTT method. For a sensitive inhibitor, both methods showed essentially the same  $IC_{50}$  and % inhibition (**Figure 5H**). When a partial inhibitor is tested, both methods showed essentially the same  $EC_{50}$  values, but % inhibition was lower in the EZMTT method, because the partially inhibited cells are still growing (**Figure 5I**). Recently, several KGA allosteric inhibitors were rediscovered as partial inhibitors. For example, CB839 had shown 100% inhibition in CTG assay [103], whereas the EZMTT assay showed approximately 80% inhibition [104], and this is further confirmed by the (DIP) rate measurement. At the steady state, 10  $\mu$ M CB839 did not completely inhibit cancer cell growth. Interestingly, when 64 nM CB839 and 24  $\mu$ M ebselen were used in combination, synergistic effects were observed; even though individual compounds only showed partial inhibition, when used in combination, nearly complete inhibition of cancer cell growth was observed [105].

As a new assay format, EZMTT showed powerful applications in cell growth analysis, clinical diagnosis of trivial drug resistance, precise medicine for drug combination, and cost-effective drug discovery by building better correlation between the in vitro cell-based assay and in vivo animal models.

## 7. Conclusions

Cell proliferation assays are widely used in molecular biology, tumor biology, pharmacology, and pharmacokinetics. It is important in studying not only the basic biological characteristics of cells but also a basic method for analyzing cell states and studying genetic traits. The increase of cell numbers can be simply measured by manual counting of cells under microscopy, using the dye exclusion method (i.e., trypan blue) to count only viable cells. Less fastidious, scalable methods include the use of cytometers; especially the flow cytometry allows combining cell counts (“events”) with other specific parameters such as fluorescent probes for membranes, cytoplasm, or nuclei which allows distinguishing dead/viable cells, cell types, cell differentiation, and expression of a biomarker such as Ki67. Beside counting the increasing number of cells, cells can also be assessed based on the metabolic activity, such as the CFDA-SE or calcein-AM method measures not only the membrane functionality (dye retention) but also the functionality of cytoplasmic enzymes (esterases). Also, the MTT-type assays or the resazurin assay (fluorimetric) measures the mitochondrial redox potential. Most of these assays are endpoint assays and may or may not correlate well with the cell proliferation, depending on cell growth conditions, populations of different cells, drug interferences, or toxicity. For precise evaluation of drug-induced proliferation rate changes, a continuous assay is highly desirable. Among various assay formats, the EZMTT dye showed initial promise in precise and sensitive detection of partial inhibition which is the cause of worldwide crisis in drug resistance, and the EZMTT method is expected to provide valuable information for exploring the pathogenesis of the disease, diagnosing the disease, and treating the disease.

## Acknowledgements

We appreciate financial support from Natural Science foundation of Zhejiang Province (Grant LY19H300002), Hangzhou Chuying grant award (H1160492), Zhejiang University of Technology (414800129), and Hangzhou qinglan grant award (H1160494).

## Conflict of interest

The authors declare no competing interests or other interests that might be perceived to influence the results and/or discussion reported in this paper.

## Notes/thanks/other declarations

We thank publishers, Cancer Letter and Experimental Cell Research, for permission of using **Figures 3** and **4**.

## Author details

Ning Xu<sup>1†</sup>, Xingrou Chen<sup>1†</sup>, Jingjing Rui<sup>1</sup>, Yan Yu<sup>1</sup>, Dongshi Gu<sup>1</sup>, Jennifer Jin Ruan<sup>2</sup> and Benfang Helen Ruan<sup>1\*</sup>

1 College of Pharmaceutical Science, Collaborative Innovation Center of Yangtze River Delta Region, IDD & CB, Green Pharmaceuticals, Zhejiang University of Technology, Hangzhou, China

2 Department of Surgery, Memorial Sloan Kettering Cancer Center, New York, NY, USA

\*Address all correspondence to: ruanbf@zjut.edu.cn; ruanbf@yahoo.com

†The authors contributed equally to this work.

## IntechOpen

© 2020 The Author(s). Licensee IntechOpen. This chapter is distributed under the terms of the Creative Commons Attribution License (<http://creativecommons.org/licenses/by/3.0>), which permits unrestricted use, distribution, and reproduction in any medium, provided the original work is properly cited. 

## References

- [1] Neumann EK, Do TD, Comi TJ, et al. Exploring the fundamental structures of life: non-targeted, chemical analysis of single cells and subcellular structures. *Angewandte Chemie-International Edition*. 2019;**58**(28):9348-9364
- [2] Shestopaloff YK. Why cells grow and divide? General growth mechanism and how it defines cells' growth, reproduction and metabolic properties. *Biophysical Reviews and Letters*. 2015;**10**(4):48-84
- [3] Ren Y, Ji Y, Teng L, et al. Using Raman spectroscopy and chemometrics to identify the growth phase of *Lactobacillus casei* Zhang during batch culture at the single-cell level. *Microbial Cell Factories*. 2017;**16**(1):233-242
- [4] Szymański P, Markowicz M, Mikiciuk-Olasik E. Adaptation of high-throughput screening in drug discovery-toxicological screening tests. *International Journal of Molecular Sciences*. 2011;**13**(12):427-452
- [5] Pariente JL, Kim BS, Atala A. In vitro biocompatibility assessment of naturally derived synthetic biomaterials using normal human urothelial cells. *Journal of Biomedical Materials Research*. 2015;**55**(1):33-39
- [6] Widlak W. Cell division. In: *Molecular Biology*. Berlin Heidelberg: Springer; 2013
- [7] Margolin W. Binary Fission in Bacteria. In: eLS. John Wiley & Sons, Ltd.; 2014
- [8] Walker MR, Rapley R. Distribution of nucleic acids within eukaryotic cells. In: *Route Maps in Gene Technology*. Wiley Blackwell; 2009:30-31
- [9] Petronczki M, Siomos MF, Nasmyth K. Un ménage à quatre: The molecular biology of chromosome segregation in meiosis. *Cell*. 2003;**112**(4):423-440
- [10] Humphrey T, Enoch T. Cell-cycle checkpoints. Keeping mitosis in check. *Current Biology*. 1995;**5**(4):376-379
- [11] Dive C, Gregory CD, Phipps DJ, et al. Analysis and discrimination of necrosis and apoptosis (programmed cell death) by multiparameter flow cytometry. *Biochimica et Biophysica Acta*. 1992;**1133**(3):275-285
- [12] Reed JC. Dysregulation of apoptosis in cancer. *The Cancer Journal from Scientific American*. 1998;**4**(9):S8
- [13] Dienstmann R, Jang IS, Bot B, et al. Database of genomic biomarkers for cancer drugs and clinical targetability in solid tumors. *Cancer Discovery*. 2015;**5**(2):118-123
- [14] Housman G, Byler S, Heerboth S, et al. Drug resistance in cancer: An overview. *Cancers*. 2014;**6**(3):1769-1792
- [15] Harris LA, Frick PL, Garbett SP, et al. An unbiased metric of antiproliferative drug effect in vitro. *Nature Methods*. 2016;**13**(6):497-500
- [16] Kodack DP, Farago AF, Dastur A, et al. Primary patient-derived cancer cells and their potential for personalized cancer patient care. *Cell Reports*. 2017;**21**(11):3298-3309
- [17] Holohan C, Van Schaeybroeck S, Longley DB, et al. Cancer drug resistance: An evolving paradigm. *Nature Reviews Cancer*. 2013;**13**(10):714-726
- [18] Gemryd P, Lundquist PG, Tytor M, et al. Prognostic significance of DNA ploidy in mucoepidermoid carcinoma. *European Archives of Oto-Rhino-Laryngology*. 1997;**254**(4):180-185
- [19] Foss S, Berner A, Jacobsen AB, et al. Clinical significance of DNA ploidy and

S-phase fraction and their relation to p53 protein, c-erbB-2 protein and HCG in operable muscle-invasive bladder cancer. *British Journal of Cancer*. 1993;**68**(3):572-578

[20] Beccia MR, Biver T, Pardini A, et al. The fluorophore 4',6-Diamidino-2-phenylindole (DAPI) induces DNA folding in long double-stranded DNA. *Chemistry-An Asian Journal*. 2012;**7**(8):1803-1810

[21] Poot M, Kavanagh TJ, Kang HC, et al. Flow cytometric analysis of cell cycle-dependent changes in cell thiol level by combining a new laser dye with hoechst 33342. *Cytometry*. 1991;**12**(2):184-187

[22] Lehtinen J, Nuutila J, Lilius EM. Green fluorescent protein-propidium iodide (GFP-PI) based assay for flow cytometric measurement of bacterial viability. *Cytometry*. 2004;**60A**(2):165-172

[23] Bellehumeur C, Boyle B, Charette SJ, et al. Propidium monoazide (PMA) and ethidium bromide monoazide(EMA) improve DNA array and high-throughput sequencing of porcine reproductive and respiratory syndrome virus identification. *Journal of Virological Methods*. 2015;**222**(6):182-191

[24] Wang L, Sun J, Horvat M, et al. Evaluation of MTS, XTT, MTT and 3 HTdR incorporation for assessing hepatocyte density, viability and proliferation. *Methods in Cell Science*. 1996;**18**(3):249-255

[25] Silva MS, Muñoz PAM, Armelin HA, et al. Differences in the detection of BrdU/EdU incorporation assays alter the calculation for G1, S, and G2 phases of the cell cycle in trypanosomatids. *Journal of Eukaryotic Microbiology*. 2017;**64**(6):756-770

[26] Bradford JA, Clarke ST. Dual-pulse labeling using 5-ethynyl-2'-deoxyuridine

(EdU) and 5-bromo-2'-deoxyuridine (BrdU) in flow cytometry. In: Robinson JP et al., editors. *Current Protocols in Cytometry*. 2011;**7**:7-38

[27] Bruno S, Darzynkiewicz Z. Cell cycle dependent expression and stability of the nuclear protein detected by Ki-67 antibody in HL-60 cells. *Cell Proliferation*. 1992;**25**(1):31-40

[28] Darzynkiewicz Z, Zhao H, Zhang S, et al. Initiation and termination of DNA replication during S phase in relation to cyclins D1, E and A, p21WAF1, Cdt1 and the p12 subunit of DNA polymerase  $\delta$  revealed in individual cells by cytometry. *Oncotarget*. 2015;**6**(14):11735-11750

[29] Baple EL, Chambers H, Cross HE, et al. Hypomorphic PCNA mutation underlies a human DNA repair disorder. *Journal of Clinical Investigation*. 2014;**124**(7):3137-3146

[30] Cowell IG, Papageorgiou N, Padget K, et al. Histone deacetylase inhibition redistributes topoisomerase IIb from heterochromatin to euchromatin. *Nucleus*. 2011;**2**(1):61-71

[31] Hendzel MJ, Wei Y, Mancini MA, et al. Mitosis-specific phosphorylation of histone H3 initiates primarily within pericentromeric heterochromatin during G2 and spreads in an ordered fashion coincident with mitotic chromosome condensation. *Chromosoma (Berlin)*. 1997;**106**(6):348-360

[32] Darzynkiewicz Z, Juan G, Li X, et al. Cytometry in cell necrobiology: Analysis of apoptosis and accidental cell death (necrosis). *Cytometry*. 2015;**27**(1):1-20

[33] Elsässer A, Vogt AM, Nef H, et al. Human hibernating myocardium is jeopardized by apoptotic and autophagic cell death. *Journal of the*

American College of Cardiology. 2004;**43**(12):2191-2199

[34] Zucker RM, Hunter S, Rogers JM. Confocal laser scanning microscopy of apoptosis in organogenesis-stage mouse embryos. *Cytometry*. 1998;**33**(3):348-354

[35] Muratori M, Forti G, Baldi E. Comparing flow cytometry and fluorescence microscopy for analyzing human sperm DNA fragmentation by TUNEL labeling. *Cytometry. Part A: The Journal of the International Society for Analytical Cytology*. 2008;**73A**(9):785-787

[36] Asher E, Payne CM, Bernstein C. Evaluation of cell death in EB V-transformed lymphocytes using agarose gel electrophoresis, light microscopy and electron microscopy: II. Induction of non-classic apoptosis ("para-apoptosis") by tritiated thymidine. *Leukemia & Lymphoma*. 1995;**19**(1-2):13

[37] Gunawan F, Nishihara J, Liu P, et al. Comparison of platform host cell protein ELISA to process-specific host cell protein ELISA. *Biotechnology and Bioengineering*. 2018;**115**:382-389

[38] Sureda FX, Escubedo E, Gabriel C, et al. Mitochondrial membrane potential measurement in rat cerebellar neurons by flow cytometry. *Cytometry*. 1997;**28**(1):74-80

[39] Engeland MV, Nieland LJW, Ramaekers FCS, et al. Annexin V-affinity assay: A review on an apoptosis detection system based on phosphatidylserine exposure. *Cytometry*. 1998;**31**(1):1-9

[40] Koç E, Çelik-Uzuner S, Uzuner U, et al. The detailed comparison of cell death detected by annexin V-PI counterstain using fluorescence microscope, flow cytometry and automated cell counter in mammalian

and microalgae cells. *Journal of Fluorescence*. 2018;**28**(6):1393-1404

[41] Zhang C, Wu R, Zhu H, et al. Enhanced antitumor activity by the combination of TRAIL/Apo-2L and combretastatin A-4 against human colon cancer cells via induction of apoptosis in vitro and in vivo. *Cancer Letters*. 2011;**302**(1):11-19

[42] Jiang X, Wang X. Cytochrome C-mediated apoptosis. *Annual Review of Biochemistry*. 2004;**73**(73):87-106

[43] Lin L, Deng W, Tian Y, et al. Lasiodin inhibits proliferation of human nasopharyngeal carcinoma cells by simultaneous modulation of the Apaf-1/caspase, AKT/MAPK and COX-2/NF- $\kappa$ B signaling pathways. *PLoS One*. 2014;**9**(5):e97799

[44] Bucevičius J, Lukinavičius G, Gerasimaitė R. The use of hoechst dyes for DNA staining and beyond. *Chem*. 2018;**6**(2):18-29

[45] Gibson B, Wilson DJ, Feil E, et al. The distribution of bacterial doubling times in the wild. *Proceedings of The Royal Society B-Biological Sciences*. 2018;**285**(1880):9

[46] Menetrez MY. An overview of algae biofuel production and potential environmental impact. *Environmental Science & Technology*. 2012;**46**(13):7073-7085

[47] Väyrynen JP, Vornanen JO, Sajanti S, et al. An improved image analysis method for cell counting lends credibility to the prognostic significance of T cells in colorectal cancer. *Virchows Archiv*. 2012;**460**:455-465

[48] Kaur C, Pal I, Saini S, et al. Comparison of unbiased stereological estimation of total number of cresyl violet stained neurons and parvalbumin positive neurons in the adult human

spiral ganglion. *Journal of Chemical Neuroanatomy*. 2018;**93**:30-37

[49] Lodeiro P, Achterberg EP, El-Shahawi MS. Detection of silver nanoparticles in seawater at ppb levels using UV-visible spectrophotometry with long path cells. *Talanta*. 2017;**164**:257-260

[50] Eltringham I, Pickering J, Gough H, et al. Comparison of mycobacterial growth indicator tube with culture on RGM selective agar for detection of mycobacteria in sputum samples from patients with cystic fibrosis. *Journal of Clinical Microbiology*. 2016;**54**(8):2047-2050

[51] Wilson ML, Weinstein MP, Reimer LG, et al. Controlled comparison of the BacT/alert and BACTEC 660/730 nanradiometric blood culture systems. *Journal of Clinical Microbiology*. 1992;**30**(2):323-329

[52] Pina-Vaz C, Costa-de-Oliveira S, Rodrigues AG. Safe susceptibility testing of mycobacterium tuberculosis by flow cytometry with the fluorescent nucleic acid stain SYTO 16. *Journal of Medical Microbiology*. 2005;**54**(1):77-81

[53] Rychtecky P, Znachor P, Nedoma J. Spatio-temporal study of phytoplankton cell viability in a eutrophic reservoir using SYTOX green nucleic acid stain. *Hydrobiologia*. 2014;**740**(1):177-189

[54] Andras SC, Hartman TPV, Alexander J, et al. Combined PI-DAPI staining (CPD) reveals NOR asymmetry and facilitates karyotyping of plant chromosomes. *Chromosome Research*. 2000;**8**(5):387-391

[55] Vichai V, Kirtikara K. Sulforhodamine B colorimetric assay for cytotoxicity screening. *Nature Protocols*. 2006;**1**(3):1112-1116

[56] Askenasy N, Farkas DL. Optical imaging of PKH-labeled hematopoietic

cells in recipient bone marrow in vivo. *Stem Cells*. 2002;**20**(6):501-513

[57] Bhowmik BB, Basu S, Ray D. Photophysical studies of 3,3'-dioctadecyloxycarbocyanine dye in model biological membranes and different solvents. *Chemistry & Physics of Lipids*. 2001;**109**(2):175-183

[58] Yumoto K, Berry JE, Taichman RS, et al. A novel method for monitoring tumor proliferation in vivo using fluorescent dye DiD. *Cytometry Part A*. 2014;**85**(6):548-555

[59] Edgardo J, Liaudat JP, Medeot D, et al. Monitoring succinoglycan production in single *Sinorhizobium meliloti* cells by Calcofluor white M2R staining and time-lapse microscopy. *Carbohydrate Polymers*. 2017;**181**:918-922

[60] Scornik FS, Bucciero RS, Wu Y, et al. DiBAC4(3) hits a "sweet spot" for the activation of arterial large-conductance Ca<sup>2+</sup>-activated potassium channels independently of the  $\beta$ 1-subunit. *AJP: Heart and Circulatory Physiology*. 2013;**304**(11):H1471-H1482

[61] Voytik-Harbin SL, Brightman AO, Waisner B, et al. Application and evaluation of the alamarblue assay for cell growth and survival of fibroblasts. *In Vitro Cellular & Developmental Biology Animal*. 1998;**34**(3):239-246

[62] O'Brien J, Orton T, Wilson I, et al. Investigation of the Alamar blue (resazurin) fluorescent dye for the assessment of mammalian cell cytotoxicity. *European Journal of Biochemistry*. 2010;**267**(17):5421-5426

[63] Mueller D, Tascher G, Damm G, et al. Real-time in situ viability assessment in a 3D bioreactor with liver cells using resazurin assay. *Cytotechnology*. 2013;**65**(2):297-305

- [64] Crouch SPM, Kozlowski R, Slater KJ, et al. The use of ATP bioluminescence as a measure of cell proliferation and cytotoxicity. *Journal of Immunological Methods*. 1993;**160**(1):81
- [65] Nilsson LE, Molin O, Anséhn S. Bioluminescent assay of bacterial ATP for rapid detection of bacterial growth in clinical blood cultures. *Journal of Bioluminescence and Chemiluminescence*. 1989;**3**(3):101-104
- [66] Angulo R, Fulcher DA. Measurement of *Candida*-specific blastogenesis: Comparison of carboxyfluorescein succinimidyl ester labelling of T cells, thymidine incorporation, and CD69 expression. *Cytometry Part A*. 2015;**34**(3):143-151
- [67] Parish CR. Fluorescent dyes for lymphocyte migration and proliferation studies. *Immunology and Cell Biology*. 1999;**77**(6):499-508
- [68] Nayla J, Claus RA, Katja D, et al. Comparative suitability of CFDA-SE and rhodamine 6G for in vivo assessment of leukocyte-endothelium interactions. *Journal of Biophotonics*. 2014;**7**(6):369-375
- [69] Kai Z, Kunpeng P, Xinyi W. Isolation and transplantation of corneal endothelial cell-like cells derived from in-vitro-differentiated human embryonic stem cells. *Stem Cells & Development*. 2014;**23**(12):1340-1354
- [70] Braut-Boucher F, Pichon J, Rat P, et al. A non-isotopic, highly sensitive, fluorimetric, cell-cell adhesion microplate assay using calcein AM-labeled lymphocytes. *Journal of Immunological Methods*. 1995;**178**(1):41-51
- [71] Legrand C, Bour JM, Jacob C, et al. Lactate dehydrogenase (LDH) activity of the number of dead cells in the medium of cultured eukaryotic cells as marker. *Journal of Biotechnology*. 1992;**25**(3):231-243
- [72] Ying W. NAD<sup>+</sup>/NADH and NADP<sup>+</sup>/NADPH in cellular functions and cell death: Regulation and biological consequences. *Antioxidants & Redox Signaling*. 2008;**10**(2):179-206
- [73] Tsang YH, Dogruluk T, Tedeschi PM, et al. Functional annotation of rare gene aberration drivers of pancreatic cancer. *Nature Communications*. 2016;**7**:10500-10510
- [74] Halliwell B. Drug antioxidant effects. A basis for drug selection? *Drugs*. 1991;**42**(4):569-605
- [75] Ramadhin C, Pillay B, Olaniran AO. Cell-based assays for IGF-I bioactivity measurement: Overview, limitations and current trends. *Growth Factors*. 2014;**32**(3-4):130
- [76] Otero AJ, Rodríguez I, Falero G. 2,3,5-triphenyl tetrazolium chloride (TTC) reduction as exponential growth phase marker for mammalian cells in culture and for myeloma hybridization experiments. *Cytotechnology*. 1991;**6**(2):137-142
- [77] Vistica DT, Skehan P, Scudiero D, et al. Tetrazolium-based assays for cellular viability: A critical examination of selected parameters affecting formazan production. *Cancer Research*. 1991;**51**(10):2515-2520
- [78] Mariana DNH, Eziefula AC, Othieno L, et al. Tools for mass screening of G6PD deficiency: Validation of the WST8/1-methoxy-PMS enzymatic assay in Uganda. *Malaria Journal*. 2013;**12**(1):210-210
- [79] Naoi T, Shibuya N, Inoue H, et al. The effect of tert-butylhydroquinone-induced oxidative stress in MDBK cells using XTT assay: Implication of tert-butylhydroquinone-induced NADPH generating enzymes. *Journal*

of Veterinary Medical Science. 2010;**72**(3):321-326

[80] Tiwari K, Wavdhane M, Haque S, et al. A sensitive WST-8-based bioassay for PEGylated granulocyte colony stimulating factor using the NFS-60 cell line. *Pharmaceutical Biology*. 2015;**53**(6):849-854

[81] Zhang W, Zhu M, Wang F, et al. Mono-sulfonated tetrazolium salt based NAD(P)H detection reagents suitable for dehydrogenase and real-time cell viability assays. *Analytical Biochemistry*. 2016;**509**:33-40

[82] Adan A, Kiraz Y, Baran Y. Cell proliferation and cytotoxicity assays. *Current Pharmaceutical Biotechnology*. 2016;**17**(14):1213-1221

[83] Riss TL, Moravec RA. Use of multiple assay endpoints to investigate the effects of incubation time, dose of toxin, and plating density in cell-based cytotoxicity assays. *Assay and Drug Development Technologies*. 2004;**2**(1):51-62

[84] Vega-Avila E, Pugsley MK. An overview of colorimetric assay methods used to assess survival or proliferation of mammalian cells. *Proceedings of the Western Pharmacology Society*. 2011;**54**:10-14

[85] Atienza JM, Zhu J, Wang X, et al. Dynamic monitoring of cell adhesion and spreading on microelectronic sensor arrays. *Journal of Biomolecular Screening*. 2005;**10**(8):795-805

[86] Giaever I, Keese CR. Monitoring fibroblast behavior in tissue culture with an applied electric field. *Proceedings of the National Academy of Sciences of the United States of America*. 1984;**81**(12):3761-3764

[87] Keese CR, Bhawe KJ, Giaever I. Real-time impedance assay to follow the invasive activities of metastatic

cells in culture. *BioTechniques*. 2002;**33**(4):842-844

[88] Caide X, Bernard L, Geoffrey S, et al. Assessment of cytotoxicity using electric cell-substrate impedance sensing: Concentration and time response function approach. *Analytical Chemistry*. 2002;**74**(22):5748-5753

[89] Xiao C, Luong JH. On-line monitoring of cell growth and cytotoxicity using electric cell-substrate impedance sensing (ECIS). *Biotechnology Progress*. 2010;**19**(3):1000-1005

[90] Wang L, Wang L, Yin H, et al. Real-time, label-free monitoring of the cell cycle with a cellular impedance sensing chip. *Biosensors & Bioelectronics*. 2010;**25**(5):990-995

[91] Keating ME, Byrne HJ. Raman spectroscopy in nanomedicine: Current status and future perspective. *Nanomedicine*. 2013;**8**(8):1335-1351

[92] Chernenko T, Sawant RR, Miljkovic M, et al. Raman microscopy for non-invasive imaging of pharmaceutical nanocarriers: Intracellular distribution of cationic liposomes of different composition. *Molecular Pharmaceutics*. 2012;**9**(4):930-936

[93] Dorney J, Bonnier F, Garcia A, et al. Identifying and localizing intracellular nanoparticles using Raman spectroscopy. *The Analyst*. 2012;**137**(5):1111

[94] El-Mashtoly SF, Petersen D, Yosef HK, et al. Label-free imaging of drug distribution and metabolism in colon cancer cells by Raman microscopy. *Analyst*. 2014;**139**(5):1155-1161

[95] Hartmann K, Becker-Putsche M, Bocklitz T, et al. A study of docetaxel-induced effects in MCF-7 cells by means of Raman microspectroscopy.

Analytical & Bioanalytical Chemistry. 2012;**403**(3):745-753

[96] Nawaz H, Garcia A, Meade AD, et al. Raman micro spectroscopy study of the interaction of vincristine with A549 cells supported by expression analysis of bcl-2 protein. *The Analyst*. 2013;**138**(20):6177

[97] Heath JR, Ribas A, Mischel PS. Single-cell analysis tools for drug discovery and development. *Nature Reviews. Drug Discovery*. 2016;**15**(3):204-216

[98] Deng R, Qu H, Liang L, et al. Tracing the therapeutic process of targeted aptamer/drug conjugate on cancer cells by surface-enhanced Raman scattering spectroscopy. *Analytical Chemistry*. 2017;**89**(5):2844-2851

[99] Oh BR, Chen P, Nidetz R, et al. Multiplexed nanoplasmonic temporal profiling of T-cell response under immunomodulatory agent exposure. *Acs Sensors*. 2016;**1**(7):941-948

[100] El-Mashtoly SF, Yosef HK, Dennis P, et al. Label-free Raman spectroscopic imaging monitors the integral physiologically relevant drug responses in cancer cells. *Analytical Chemistry*. 2015;**87**(14):7297-7304

[101] Farhane Z, Bonnier F, Howe O, et al. Doxorubicin kinetics and effects on lung cancer cell lines using in vitro Raman micro-spectroscopy: Binding signatures, drug resistance and DNA repair. *Journal of Biophotonics*. 2018;**11**(1):14

[102] Zhu M, Fang J, Zhang J, et al. Biomolecular interaction assays identified dual inhibitors of glutaminase and glutamate dehydrogenase that disrupt mitochondrial function and prevent growth of cancer cells. *Analytical Chemistry*. 2017;**89**:1689-1696. DOI: 10.1021/acs.analchem.6b03849

[103] Gross MI, Demo SD, Dennison JB, et al. Antitumor activity of the glutaminase inhibitor CB-839 in triple-negative breast cancer. *Molecular Cancer Therapeutics*. 2014;**13**:890-901

[104] Chen Z, Li D, Xu N, et al. Novel 1,3,4-selenadiazole-containing kidney-type glutaminase inhibitors showed improved cellular uptake and antitumor activity. *Journal of Medicinal Chemistry*. 2019;**62**(2):589-603. DOI: 10.1021/acs.jmedchem.8b01198

[105] Ruan JJ, Yu Y, Hou W, et al. Kidney type glutaminase inhibitor hexylselen selectively kills cancer cells via a three-pronged mechanisms. *ACS Pharmacology & Translational Science*. 2019;**2**(1):18-30